RSC Advances

RSC Publishing

COMMUNICATION

View Article Online
View Journal | View Issue

Phase investigation on zinc–tin composite crystallites†

Dawei Wang, Wenbo Wang, Zhe Zhu, Peng Sun,* Jian Ma and Geyu Lu*

Cite this: *RSC Advances*, 2013, **3**, 12084

Received 12th April 2013,
Accepted 23rd May 2013

DOI: 10.1039/c3ra41767k

www.rsc.org/advances

Zinc–tin composite crystallites (cubes and octahedra) synthesized by conventional methods in earlier literature, were proved to have $ZnSn(OH)_6$ structures rather than perovskite structure $ZnSnO_3$ as reported. Furthermore, according to the tolerance factor *t* introduced by Goldschmidt, $ZnSnO_3$ can not exist as a perovskite structure.

Zinc stannate, as a ternary semiconducting metal oxide, has received much attention in the past decade. Thus, various methods[1–6] have been applied to prepare zinc stannate to obtain different morphologies. According to most investigators' viewpoints, zinc stannate exists as two types of oxides with different Zn/Sn/O ratios and crystallographic structures: the spinel-type cubic Zn_2SnO_4 and the perovskite $ZnSnO_3$.[7] Spinel Zn_2SnO_4 synthesized by various methods has been proved to have a stable and certain state,[8] nevertheless the data for the perovskite $ZnSnO_3$ are contradictory and ambiguous. Recently, so-called perovskite $ZnSnO_3$ structures were synthesized by some groups. For example, Baoyou Geng *et al.*[9] presented a process for the synthesis of octahedral, truncated octahedral, and 14-faceted polyhedral $ZnSnO_3$ microcrystals at low temperature (85 °C). Yi Zeng *et al.*[10] have prepared cubic $ZnSnO_3$ nanocages with hierarchical architectures *via* a hexamethylenetetramine (HMT) assisted hydrothermal process. Masahiro Miyauchi *et al.*[11] synthesized single crystalline $ZnSnO_3$ nanoparticles by a simple one-step hydrothermal reaction. Guanxiang Ma *et al.*[12] have reported a pure-phase synthesis of well-defined faceted cubic $ZnSnO_3$ microcrystals in a hydrothermal synthesis. It is worth noting that all the so-called $ZnSnO_3$ powders had a small peak at $2\theta = 43.5^\circ$ in their XRD patterns,[9–12] however, in the standard spectrum of the perovskite $ZnSnO_3$ structure (JCPDS No. 11-0274), such a small diffraction peak can not be found. On the other hand, this small peak at $2\theta = 43.5^\circ$ can be found in the standard spectrum of the $ZnSn(OH)_6$ structure (JCPDS No. 73-2384), for which most of the main diffraction peaks are the same as those of the perovskite $ZnSnO_3$ (JCPDS No. 11-0274) except for this small peak. In this work, a series of experiments (refer to ref. 9 and 12) and analyses were carried out to identify the phase of the as-synthesized zinc–tin composite crystallites. Our results indicate that these composite crystallites are the $ZnSn(OH)_6$ structures rather than the perovskite $ZnSnO_3$ as reported.

All the reagents in the experiment were of analytical grade and were used without further purification. The cubic and octahedral crystallites were prepared using the same synthetic methods and conditions (raw materials, solution concentration and experimental conditions) as those in ref. 12 and 9, respectively, except for the suppliers of the raw materials (see the ESI† for the experimental details). The X-ray diffraction (XRD) patterns were recorded on a Rigaku D/Max-2500 diffractometer with CuKα radiation (λ = 1.5406 Å). Field emission scanning electron microscopy (FESEM) observations were carried out using a JEOL JSM-7500F microscope with an accelerating voltage of 15 kV. Thermogravimetric (TG) analysis and differential scanning calorimetric (DSC) measurements were carried out with a NETZSCH STA 449F3 simultaneous thermogravimetric analyzer under air in the temperature range 30 °C to 800 °C, with a heating rate of 10 °C min^{-1}. The FTIR spectra were recorded on a Nicolet 6700 Fourier transform infrared spectrometer, at wavenumbers 400–4000 cm^{-1} using KBr pellets.

Fig. 1(a) and (b) show the SEM images of the as-obtained cubic and octahedral crystallites in our experiment. It can be seen that their morphologies are similar to those presented in Fig. 1(d) and (f), respectively, which were copied from ref. 12 and 9 directly for a comparison. Fig. 1(c) shows the XRD patterns of the as-obtained cubic and octahedral samples. All of the diffraction peaks can be indexed to the cubic $ZnSn(OH)_6$ with the calculated lattice parameter a = 7.80 Å, which is in good agreement with the literature value (JCPDS No. 73-2384), including the small peak (321) at $2\theta = 43.5^\circ$, labeled in the figure with a red rectangle. No other crystalline phases or obvious peaks of impurities were detected. Fig. 1(e) and (g) show the XRD patterns of the cubic and octahedral samples prepared by the authors of ref. 12 and 9. They thought that their as-synthesized products were the pure-phase

State Key Laboratory on Integrated Optoelectronics, College of Electronic Science and Engineering, Jilin University, Changchun 130012, People's Republic of China. E-mail: spmaster2008@163.com; Fax: +86 431 85167808; Tel: +86 431 85167808

† Electronic supplementary information (ESI) available: Experimental details, TG and DSC curves, phase transition and FTIR data of the octahedral crystallites. See DOI: 10.1039/c3ra41767k

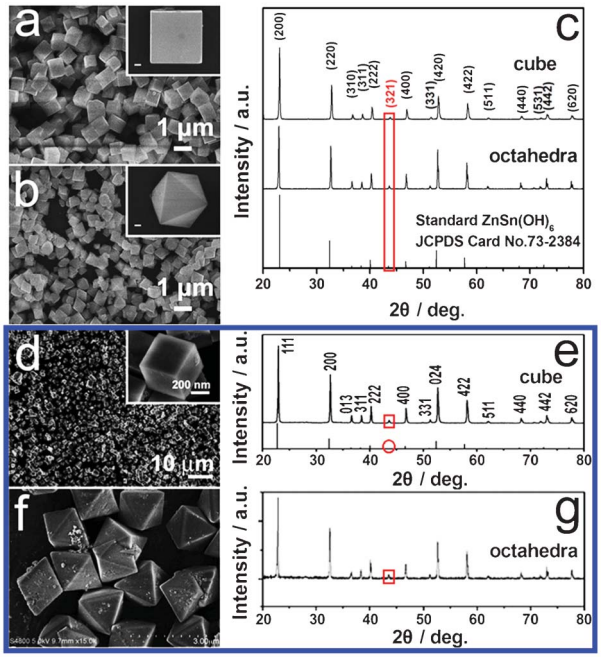

Fig. 1 SEM images for (a) cubic and (b) octahedral crystallites; XRD patterns (c) of the as-obtained cubic crystallites, octahedral crystallites and the standard XRD pattern of $ZnSn(OH)_6$ (JCPDS No. 73-2384). The insets of (a) and (b) show the corresponding high magnification images with a scale bar of 100 nm. SEM image (d) and XRD pattern (e) for the cubic crystallites from ref. 12, SEM image (f) and XRD pattern (g) for the octahedral crystallites from ref. 9, as circumscribed in the blue frame.

perovskite $ZnSnO_3$ structures (JCPDS No. 11-0274). However, it is clear that there is a small diffraction peak at $2\theta = 43.5^\circ$ in the XRD of their products, while such a small peak does not exist in the standard spectrum of the so-called perovskite $ZnSnO_3$ structure (JCPDS No. 11-0274) as shown in Fig. 1(e) with a red circle. Contrarily, this is the same as our results; the XRD patterns can be indexed to the standard $ZnSn(OH)_6$ structure (JCPDS No. 73-2384), including the small peak at $2\theta = 43.5^\circ$. Based on the above analysis, these zinc–tin composite crystallites may be not perovskite $ZnSnO_3$, but $ZnSn(OH)_6$ structures.

In order to validate our point of view, thermogravimetric (TG) and differential scanning calorimetric (DSC) measurements were carried out under air in the temperature range 30 °C to 800 °C, with a heating rate of 10 °C min^{-1}. The TG and DSC curves of the as-obtained cubic crystallites are shown in Fig. 2. If the samples are perovskite $ZnSnO_3$ structures, there should be only a small weight loss, caused by the physisorbed water in the air. However, if the samples are $ZnSn(OH)_6$ structures, there should be a dehydration procedure ($2ZnSn(OH)_6 \rightarrow Zn_2SnO_4 + SnO_2 + 6H_2O$) through the heating treatment, with a theoretical proportion of 18.88% for $3H_2O$ in the $ZnSn(OH)_6$. It can be seen that the TG curve presents an obvious weight loss stage, of about 18.6%, in the temperature range 200 °C–400 °C, as shown in Fig. 2. This matches the theoretical weight loss value in the dehydration process of $ZnSn(OH)_6$. This result further proves the fact that a mass of hydroxyl groups exists in the as-obtained samples. These

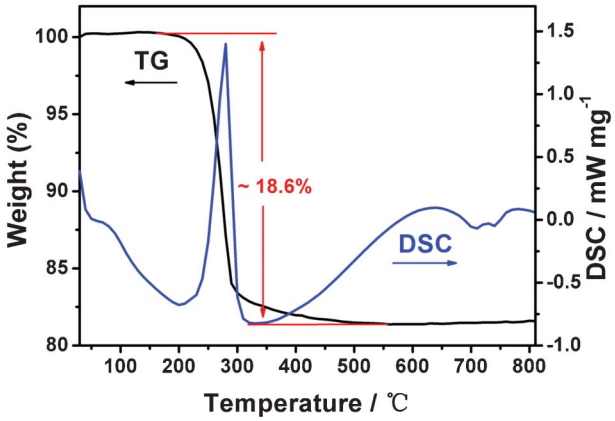

Fig. 2 TG and DSC curves of the as-obtained cubic crystallites in air.

crystallites are not $ZnSnO_3$ but $ZnSn(OH)_6$ structures. The DSC curve exhibits an endothermic peak at 280 °C, which can be attributed to the weight loss stage. In addition, there are several exothermic peaks between 600 °C and 800 °C, which can possibly be attributed to the phase transition process. This point will be confirmed by the XRD patterns of the samples annealed at different temperatures (Fig. 4).

FTIR spectra were then recorded in the range 400–4000 cm^{-1} using KBr pellets, to further verify the existence of hydroxyl groups in the as-obtained samples. Fig. 3 displays the FTIR spectra of vacuum oven dried cubic crystallites before being annealed, annealed at 200 °C and annealed at 700 °C. Furthermore, the FTIR spectra of pure Zn_2SnO_4 and SnO_2 are also presented for comparison. Pure Zn_2SnO_4 and SnO_2 were obtained according to the literature.[12,13] It is specially noted that the samples were pre-treated in a vacuum oven at 100 °C for 12 h, just before recording the FTIR spectra, to remove the physisorbed water on the surface of the samples. From Fig. 3, it can obviously be seen that the strong peak at 3159 cm^{-1} of the cubic crystallites before being

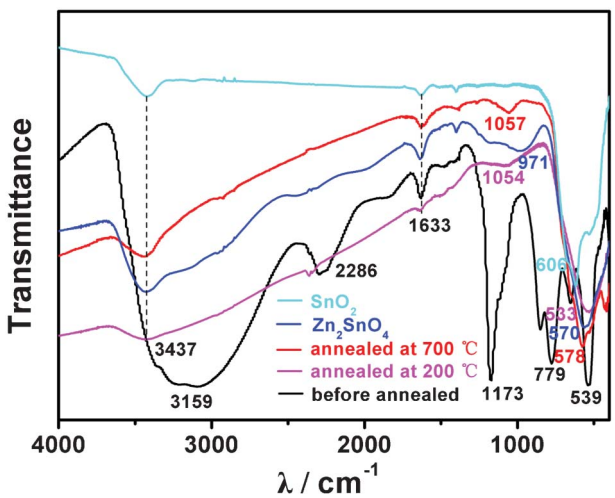

Fig. 3 FTIR spectra of the vacuum oven dried cubic crystallites before being annealed, annealed at 200 °C, annealed at 700 °C, pure Zn_2SnO_4 and SnO_2.

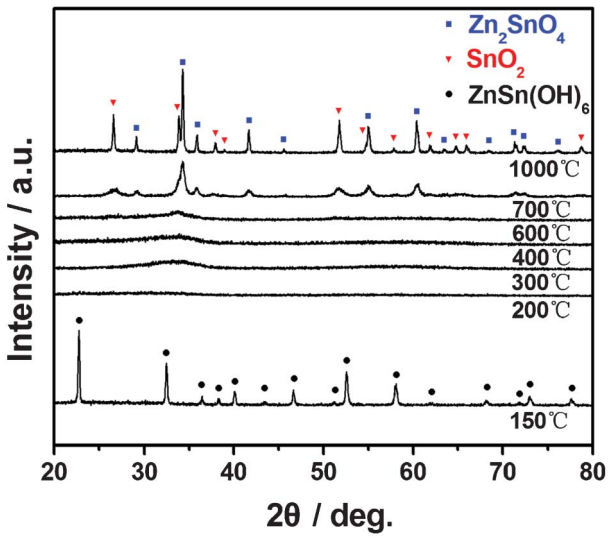

Fig. 4 XRD patterns of the cubic crystallites annealed in air at different temperatures from 150 °C to 1000 °C.

annealed can be attributed to an O–H stretching, which agrees with the literature available on hydroxides, where the hydroxyl ion is among the main components of the structural units of minerals and synthetic hydroxides.[14] The weak peak at 3437 cm^{-1} of the other four curves can be attributed to the physisorbed H_2O molecules on the crystallites surface. This significant difference in the FTIR spectra strongly proves the existence of the hydroxyl groups in the as-synthesized samples again. The peaks observed at wave numbers 2286 cm^{-1}, 1173 cm^{-1}, 779 cm^{-1} and 539 cm^{-1} may be attributed to the vibration of the M–OH or M–OH–M groups for the structure of $ZnSn(OH)_6$. The peaks at 1057 cm^{-1} and 578 cm^{-1} may be attributed to the vibration of the M–O or M–O–M groups for SnO_2–Zn_2SnO_4.[15] For pure Zn_2SnO_4 and SnO_2, the peaks at 570 cm^{-1}, 606 cm^{-1} and 971 cm^{-1} can be attributed to the vibration of the M–O group. Moreover, the small peaks at 1633 cm^{-1} in these five spectra can be attributed to the bending vibration and stretching vibration modes of the hydroxyl group in the physisorbed H_2O molecules.[16]

To investigate the phase transition process and explore whether we obtained the pure-phase perovskite $ZnSnO_3$ structure, the as-synthesized samples were annealed in air in a muffle furnace at different temperatures. The XRD patterns of the cubic crystallites annealed in air from 150 °C to 1000 °C are shown in Fig. 4. When the samples were annealed at 150 °C, the diffraction peaks can still be indexed to the standard $ZnSn(OH)_6$ structure (JCPDS No. 73-2384). However, when the annealing temperature was varied in the range 200–600 °C, the samples became amorphous. When the annealing treatment was carried out at 700 °C, the sample became a complex phase, which can be indexed to the standard XRD patterns of Zn_2SnO_4 (JCPDS No. 24-1470) and SnO_2 (JCPDS No. 41-1445) without the relative intensity variation and impurity peaks, as marked in Fig. 4 with different signs (see Fig. S2(b) in the ESI† for details). When the annealing temperature was raised to 1000 °C, the diffraction peaks of the complex phase were more obvious. It is noteworthy that the perovskite $ZnSnO_3$ structure (JCPDS No. 11-0274) did not appear in this whole process. These results further confirm our viewpoint that the as-prepared products were the $ZnSn(OH)_6$ structures rather than the perovskite $ZnSnO_3$. Moreover, Goldschmidt[17] introduced the tolerance factor t to describe the characteristic distortion of an ABO_3 perovskite structure, $t = (R_A + R_O)/\sqrt{2}\,(R_B + R_O)$, where R_A, R_B and R_O are the ionic radii of A, B and O, respectively. For ABO_3 to exist as a perovskite structure, t must be in the range $0.77 < t < 1.1$. The tolerance factor t is just about 0.72 for $ZnSnO_3$, with the ionic radii of Zn^{2+} (0.74 Å), Sn^{4+} (0.71 Å) and O^{2-} (1.4 Å). From this point of view, $ZnSnO_3$ can not exist as a perovskite structure since the ionic radius of Zn^{2+} is too small.

The TG, DSC (see ESI,† Fig. S1), XRD (see ESI,† Fig. S2) and FTIR (see ESI,† Fig. S3) data of the octahedral crystallites are similar to those of the above-mentioned cubic crystallites, which demonstrates the fact that hydroxyl groups exist in the as-synthesized products. This proves that the zinc–tin composite crystallites are the $ZnSn(OH)_6$ structures rather than the perovskite $ZnSnO_3$.

In summary, zinc–tin composite crystallites (cubic and octahedral crystallites) were prepared by conventional methods, refer to ref. 12 and 9, respectively. From the XRD, TG, DSC and FTIR analyses, it has been proved that these composite crystallites are not the perovskite $ZnSnO_3$ but $ZnSn(OH)_6$ structures. This viewpoint is different from the previous reports. Furthermore, these hydroxides, when they were annealed in the range 150 °C–1000 °C, were changed from the $ZnSn(OH)_6$ structure to an amorphous material at 200 °C and to a SnO_2–Zn_2SnO_4 complex phase at 700 °C. It is worth noting that the perovskite $ZnSnO_3$ structure did not appear in the whole annealing process.

This work was supported by the National Nature Science Foundation of China (No. 61074172, 61134010 and 61006055), the Program for Chang Jiang Scholars and Innovative Research Team in University (No. IRT1017) and the "863" High Technology Project (2013AA030902). Project (20121105) was supported by the Graduate Innovation Fund of Jilin University.

Notes and references

1 N. Nikolić, T. Srećković and M. M. Ristić, *J. Eur. Ceram. Soc.*, 2001, **21**, 2071–2074.
2 G. Fu, H. Chen, Z. Chen, J. Zhang and H. Kohler, *Sens. Actuators, B*, 2002, **81**, 308–312.
3 J. X. Wang, S. S. Xie, Y. Gao, X. Q. Yan, D. F. Liu, H. J. Yuan, Z. P. Zhou, L. Song, L. F. Liu, W. Y. Zhou and G. Wang, *J. Cryst. Growth*, 2004, **267**, 177–183.
4 D. Kovacheva and K. Petrov, *Solid State Ionics*, 1998, **109**, 327–332.
5 H. Chen, J. Wang, H. Yu, H. Yang, S. Xie and J. Li, *J. Phys. Chem. B*, 2005, **109**, 2573–2577.
6 J. Fang, A. Huang, P. Zhu, N. Xu, J. Xie, J. Chi, S. Feng, R. Xu and M. Wu, *Mater. Res. Bull.*, 2001, **36**, 1391–1397.
7 X. Y. Liu, H. W. Zheng, Z. L. Zhang, X. S. Liu, R. Q. Wan and W. F. Zhang, *J. Mater. Chem.*, 2011, **21**, 4108–4116.
8 S. Baruah and J. Dutta, *Sci. Technol. Adv. Mater.*, 2011, **12**, 013004–013021.
9 B. Geng, C. Fang, F. Zhan and N. Yu, *Small*, 2008, **4**(9), 1337–1343.

10 Y. Zeng, T. Zhang, H. T. Fan, W. Y. Fu, G. Y. Lu, Y. M. Sui and H. B. Yang, *J. Phys. Chem. C*, 2009, **113**, 19000–19004.
11 M. Miyauchi, Z. F. Liu, Z. G. Zhao, S. Anandan and K. Hara, *Chem. Commun.*, 2010, **46**, 1529–1531.
12 G. Ma, R. Zou, L. Jiang, Z. Zhang, Y. Xue, L. Yu, G. Song, W. Liand and J. Hu, *CrystEngComm*, 2012, **14**, 2172–2179.
13 P. Sun, Y. Cao, J. Liu, Y. F. Sun, J. Ma and G. Y. Lu, *Sens. Actuators, B*, 2011, **156**, 779–783.
14 K. Beckenkamp and H. D. Lutz, *J. Mol. Struct.*, 1992, **270**, 393–405.
15 M. Wu, X. Li, G. Shen, J. Li, R. Xu and D. M. Proserpio, *J. Solid State Chem.*, 2000, **151**, 56–60.
16 J. Zeng, M. D. Xin, K. W. Li, H. Wang, H. Yan and W. J. Zhang, *J. Phys. Chem. C*, 2008, **112**, 4159–4167.
17 V. M. Goldschmidt, *Geochemische Verteilungsgesetze der Elemente VII, VIII*, 1927.